Forces on Zonal Flows in Tokamak Core Turbulence

K. Hallatschek
Centre for Interdisciplinary Plasma Physics, Max-Planck-Institut für Plasmaphysik, EURATOM Association, D-85748 Garching, Germany
E-mail: hallatschek@ipp.mpg.de
K. Itoh
National Institute for Fusion Science, Toki 509-5292, Japan
Abstract. The saturation of stationary zonal flows (ZF) in the core of a tokamak has been analyzed in numerical fluid turbulence computer studies. The model was chosen to properly represent the kinetic global plasma flows, i.e., undamped stationary toroidal or poloidal flows and Landau damped geodesic acoustic modes. Reasonable agreement with kinetic simulations in terms of magnitude of transport and occurance of the Dimits shift was verified. Contrary to common perception, in the final saturated state of turbulence and ZFs, the customary perpendicular Reynolds stress continues to drive the ZFs. The force balance is established by the essentially quasilinear parallel Reynolds stress acting on the parallel return flows required by incompressibility.

1 Introduction

It is now common knowledge that the saturation of the ion turbulence in the core of magnetic fusion devices at mixing length estimates crucially requires the presence of zonal flows (ZF), radially localized but poloidally and toroidally homogeneous electric fields, which correspond to a poloidal rotation of a flux surface as a whole [1, 2, 3]. Artificially switching off the ZFs in nonlinear turbulence computations results in a transport increase by up to two orders of magnitude. The ZFs themselves are assumed to be excited by the turbulence, i.e., by its perpendicular Reynolds stress accumulating poloidal momentum at certain (minor) radial positions. Knowledge about the ZFs is not only important for an understanding of standard tokamak or stellarator turbulence, but seems to be linked to the shear flows observed upon transitions into improved confinement regimes, like the H-mode or internal transport barriers.

Different from the core, in the edge of a tokamak, the ZFs have been shown in the past to take the form of oscillating geodesic acoustic modes [4], since the poloidal rotation of the curved torus is not free of divergence, but contains regions, where the plasma is compressed while moving towards lower major radii or decompressed while moving to increasing major radii. The compression and expansion consume free energy, which necessarily has to be taken from the kinetic energy of the rotation: a restoring force ensues, resulting in an oscillation.

Since the core ZFs are known to be quasi-stationary from turbulence simulations, additional auxiliary flows parallel to the magnetic field must exist which cancel their inherent divergence. The auxiliary flows occur whenever the poloidal $\boldsymbol{E} \times \boldsymbol{B}$ velocity has a divergence, i.e., for all types of magnetic equilibria with finite geodesic curvature. They are thus not restricted to tokamaks, but would occur in such exotic situations as, e.g., flows within solar flares. Studies of generation and saturation [1, 2, 3, 5, 6] of poloidal ZFs in the core of tokamaks have considered the radial transport of poloidal momentum, i.e., the perpendicular Reynolds stress alone, despite the obvious necessity of the auxiliary parallel flows to render the poloidal flow stationary.

The numerical turbulence simulations and analytical discussions in the present paper deal with the complete force balance on the ZFs including the auxiliaray flows, the auxiliary flows' magnitude, their interaction with the turbulence, and the reason for the difference between core and edge ZFs.

2 Core turbulence model equations

For the numerical and analytical computations, we intentionally use the most simple model complete enough to encompass the essential physics (ion temperature gradient (ITG) modes, undamped stationary ZFs, undamped toroidal flows, and linearly damped oscillating geodesic acoustic modes). These requirements essentially single out the electrostatic 3D two-fluid equations. We use variants of the 3D ITG fluid equations in [7] derived with the additional approximations of adiabatic electrons (due to the high electron thermal velocity) and local conditions (due to low $\rho^* = \rho_i/a$). In dimensionless units, the system for the fluctuation quantities $\phi, T_{\rm i}, v_\parallel$ is

$$D_t[(1-2{\nabla_\perp}^2)(\phi-\langle\phi\rangle)-{\nabla_\perp}^2\langle\phi\rangle]+\partial_y\phi-\nabla_\perp\cdot D_t\nabla_\perp T_{\rm i}$$

$$-\epsilon_n\hat{\rm C}\left[2\phi-\langle\phi\rangle+T_{\rm i}\right]+\epsilon_v\partial_\parallel v_\parallel=0, \tag{1}$$

$$D_t[T_{\rm i}-\frac{2}{3}(\phi-\langle\phi\rangle)]+\left(\eta_{\rm i}-\frac{2}{3}\right)\partial_y\phi-\frac{5}{3}\epsilon_n\hat{\rm C}T_{\rm i}=\frac{2}{3}\kappa_{\rm i}\partial_\parallel^2 T_{\rm i}, \tag{2}$$

$$D_t v_\parallel=-\epsilon_v\partial_\parallel(2\phi+T_{\rm i}). \tag{3}$$

The background electron and ion temperatures are equal and the ions are singly charged. Gradient lengths are defined as $L_\xi = d\ln r/d\ln\xi$, $\xi = n_0, T_{\rm i0}$. The parallel co-ordinate $z\equiv\theta$ ranges from $-\pi\ldots\pi$, i.e., the parallel length unit is $L_\parallel = qR$. The perpendicular co-ordinates x, y are given in ion gyro radii $\rho_{\rm i} = \sqrt{m_{\rm i}T_{\rm i0}}/(eB)$. The unit for the electric potential energy $e\phi$ and ion temperature is $T_{\rm i0}\rho_{\rm i}/L_n$. With the ion sound velocity $c_{\rm S} = \sqrt{T_{\rm i0}/m_{\rm i}}$ the parallel and perpendicular velocity unit is $v_{\rm di} = c_{\rm S}\rho_{\rm i}/L_n$, which makes the time unit $t_0 = L_n/c_{\rm S}$. The dimensionless parameters are $\epsilon_n = 2L_n/R$, $\eta_{\rm i} = L_n/L_{\rm Ti}$, $\epsilon_v = \epsilon_n/(2q) = L_n/(qR)$ (the parallel sound speed c_s in terms of $L_\parallel/t_0$, which differs from the parallel velocity unit), $\kappa_{\rm i}$ is the parallel heat conductivity. To obtain damping rates for the parallel ion temperature fluctuations similar to those from kinetic phase mixing, $\kappa_{\rm i}$ for the equilibrium perturbations $k_y = 0$ (for the turbulence $k_y > 0$ modes) is chosen, so that temperature perturbations with a typical parallel wavenumber $k_\parallel = 1$ (~ 4 for the turbulence modes) are damped at the sound frequency, i.e., $\kappa_{\rm i} = 3/2\epsilon_v$ ($\kappa_{\rm i} = 3/8\epsilon_v$). The advective time derivative D_t is $\partial_t + \hat{z}\times\nabla_\perp\phi\cdot\nabla_\perp$, the curvature terms are computed for circular geometry $\hat{\rm C} = \cos z\partial_y + \sin z\partial_x$, and the derivative along the magnetic field, $\partial_\parallel$ is $\partial_z - sx\partial_y$ taking into account the magnetic shear s. The contributions of the flux surface average $\langle\phi\rangle$ in the equations assure that the electrons do not react adiabatically to homogeneous ϕ fluctuations on a flux surface, thus allowing for ZFs. The ITG modes in the above system have been examined in [8].

3 Linear flow properties

The toroidal stationary flows are represented by $v_\parallel(y,z) = \text{const}$ and $\phi = T_{\rm i} = 0$. They are stationary in the above system, since it contains only derivatives of $v_\parallel$ with respect to the parallel co-ordinate.

A poloidal ZF has an electric potential homogeneous on a flux surface, $\phi = \langle\phi\rangle$. For stationary flows, the finite radial gradients of the ZF's electric potential occuring in the curvature term in Eq. 1, $-\epsilon_n \hat{\mathrm{C}}[2\phi - \langle\phi\rangle] = -\epsilon_n \hat{\mathrm{C}}\phi = -\epsilon_n \sin\theta \partial_x \phi$, have to be balanced by a parallel velocity field of the form $v_\| = -\epsilon_n/\epsilon_v \phi \cos\theta$. Finally, the oscillating GAMs couple all three fields and are damped by dissipation. They can be readily derived for low sound velocity, dissipation and radial wavenumber $\kappa_{\mathrm{i}}, \epsilon_v, k_x \rightarrow 0$. In that limit, $\phi = \langle\phi\rangle(1 + k_x \sin\theta/\omega)(1 + O(k_x^2))$, $T_{\mathrm{i}} = 2/3\langle\phi\rangle(k_x \sin\theta/\omega)(1 + O(k_x^2))$, and frequency $\omega = 4/3\epsilon_n$. For the actually used $\kappa_{\mathrm{i}}, \epsilon_v$ the GAM frequency is shifted somewhat due to the coupling to the parallel velocity, and (for core parameters) it is damped in about a sound transit time by the fluid heat conduction term, as it is in the kinetic system by Landau damping [9].

Thus both the required ingredients, undamped stationary ZFs [10] and geodesic acoustic modes (GAM) [4, 11], are supported.

The total kinetic energy density of the stationary ZF, including the return flow, is

$$E(v_y) = \frac{1}{2}(\langle {v_\|}^2\rangle + \langle v_y^2\rangle) = (1 + 2q^2)\frac{\langle v_y\rangle^2}{2}. \tag{4}$$

Since in practical cases $q > 1$, the major part of the kinetic energy is hidden in the return flow. In other words, the poloidal flows experience an effective mass density enhanced by the factor $1 + 2q^2$ [12]. A similar enhancement arises in the gyrokinetic collisionless analysis with circular flux surfaces of low inverse aspect ratio $\epsilon = a/R$, where the factor is increased to $1 + 1.6q^2/\sqrt{\epsilon}$ [10] owing to the additional free energy contained in the non-Maxwellian features of the auxiliary flow [13].

From the mode structure and energy conservation one can immediately obtain the rate of change of the ZFs,

$$\partial_t v_y = \frac{\langle f_y - 2q\cos(\theta) f_\| \rangle}{1 + 2q^2}, \tag{5}$$

where the poloidal and parallel force densities $f_y, f_\|$ are given by the negative divergence of the respective Reynolds stresses. Apparently, the most important term is not the flux surface averaged poloidal force $\langle f_y\rangle = -\partial_x R_{\mathrm{p}}$ since it is weakened by the neoclassical factor, but instead the in/out asymmetry of the parallel force $\langle f_\| \cos\theta\rangle = -\partial_x R_\|$ produced by the appropriate average $R_\| = \langle\cos(\theta) v_\| v_x\rangle$ of the parallel Reynolds stress. $R_{\mathrm{p}}, R_\|$ correspond exactly to the even and odd source terms of the gyrokinetic theory in [10], respectively.

From these linear considerations one can expect that, due to its dominance, turbulent radial diffusion of the parallel return flow should play a vital role in controlling the ZF level.

4 Nonlinear turbulence computations

The interplay of perpendicular and parallel turbulent forces on the ZFs has been explored in a series of numerical studies of toroidal ion temperature gradient (ITG) turbulence, centered around the well known cyclone base case parameter set [14], $\epsilon_n = 0.9$, $s = 0.8$, $R/L_n = 2.22$, $\eta_{\mathrm{i}} = 3.1$, $q = 1.4$. Average computational domain sizes of $130\rho_{\mathrm{i}} \times 2000\rho_{\mathrm{i}} \times 2\pi L_\|$ at a grid resolution of $128 \times 2048 \times 32$ were used. Corroborating the model, the threshold temperature gradient and the transport at the base case parameters agree to

30% with the gyrokinetic results. Moreover the nonlinear upshift of the threshold known from gyrokinetic models [14] occurs in the fluid model, too.

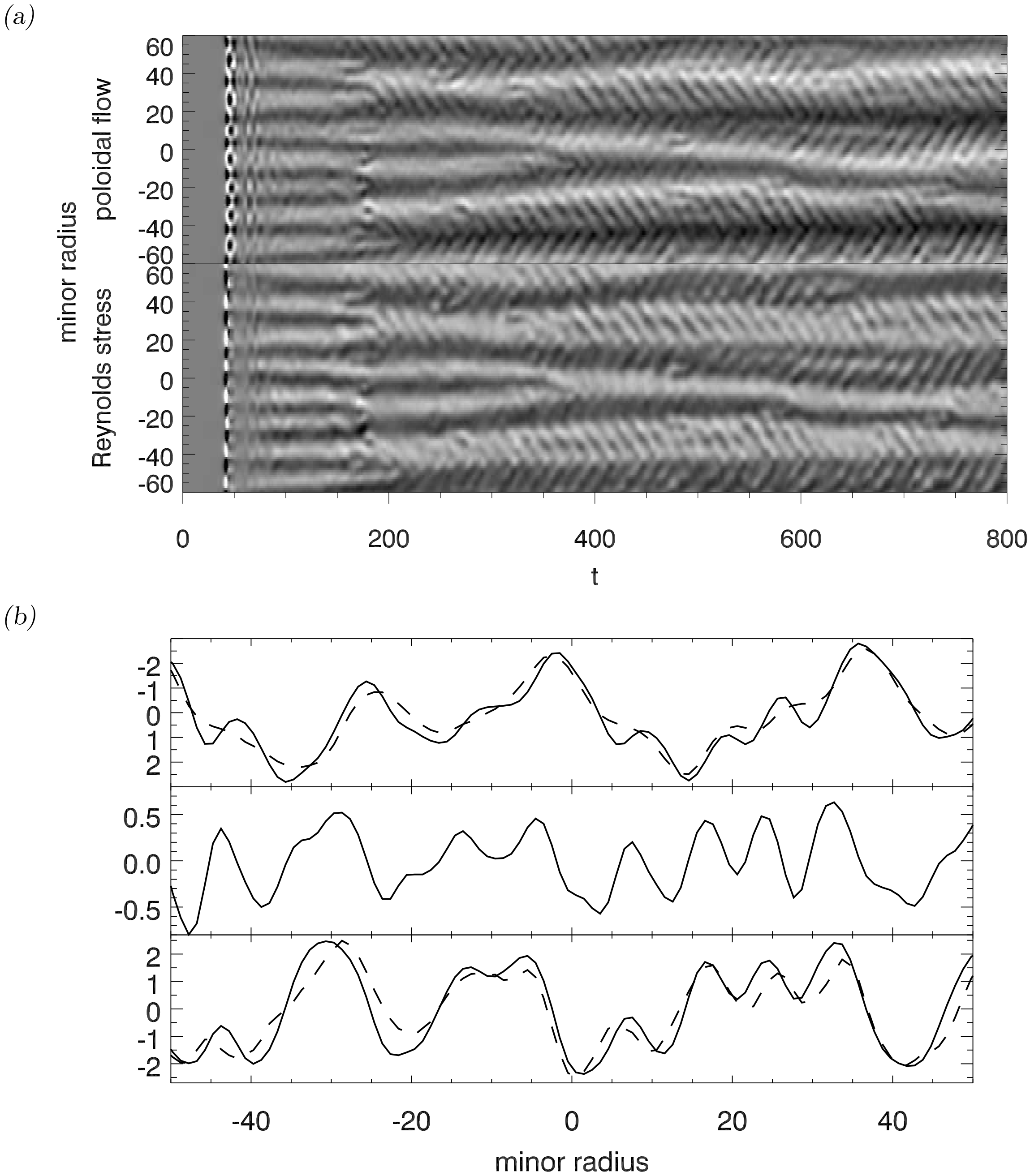

Fig. 1. Results of turbulence computation with cyclone base case parameters; a) poloidal flow versus radial position and time; b) Flux surface averages versus radius in dimensionless units at $t = 710$. Solid: poloidal flow (upper plot), shearing rate (middle plot), poloidal Reynolds stress (lower plot). Dashed: return flow (upper plot), negative parallel stress (lower plot). Note the good balance between poloidal and parallel return flow and poloidal and parallel stress, respectively. The poloidal stress is in phase with the shearing rate and is thus driving.

For gradients above the nonlinear ITG threshold, stationary zonal flows are generated and their amplitude evolves into a nearly stationary state (see, e.g., fig. 1a). In addition oscillating GAMs are also observed. They are believed to play a minor role in the determination of the turbulence level [11]. (For small computation domain widths in y, e.g., the $130\rho_\mathrm{i} \times 130\rho_\mathrm{i} \times 2\pi L_\parallel$, the flows are much more irregular at a somewhat reduced transport. This is a finite ρ^* effect due to the fluctuating part of the Reynolds stress [15].)

The stationary flows are well described by the linear modes discussed above. A comparison of the solid and dashed curves in the upper third of fig. 1b) shows the poloidal $\boldsymbol{E} \times \boldsymbol{B}$ flow to be accurately matched by the parallel return flow rescaled by ϵ_v/ϵ_n.

Different from previously proposed saturation mechanisms [1], the customary perpendicular Reynolds stress continues to heavily drive the ZFs, even in the saturated phase. Comparing the measured perpendicular Reynolds stress, shown as the solid curve in the lower third of fig. 1b), with the flow shear (middle plot in the same figure) one finds that the flow would continue to grow with the rather short time constant 0.25 if the perpendicular stress was the only force. In reality, the flows are prevented from growing further by the braking due to the turbulent advection of the parallel flow component. The effective perpendicular and parallel stresses are compared in the lower third of fig. 1 b) and obviously cancel each other quite accurately.

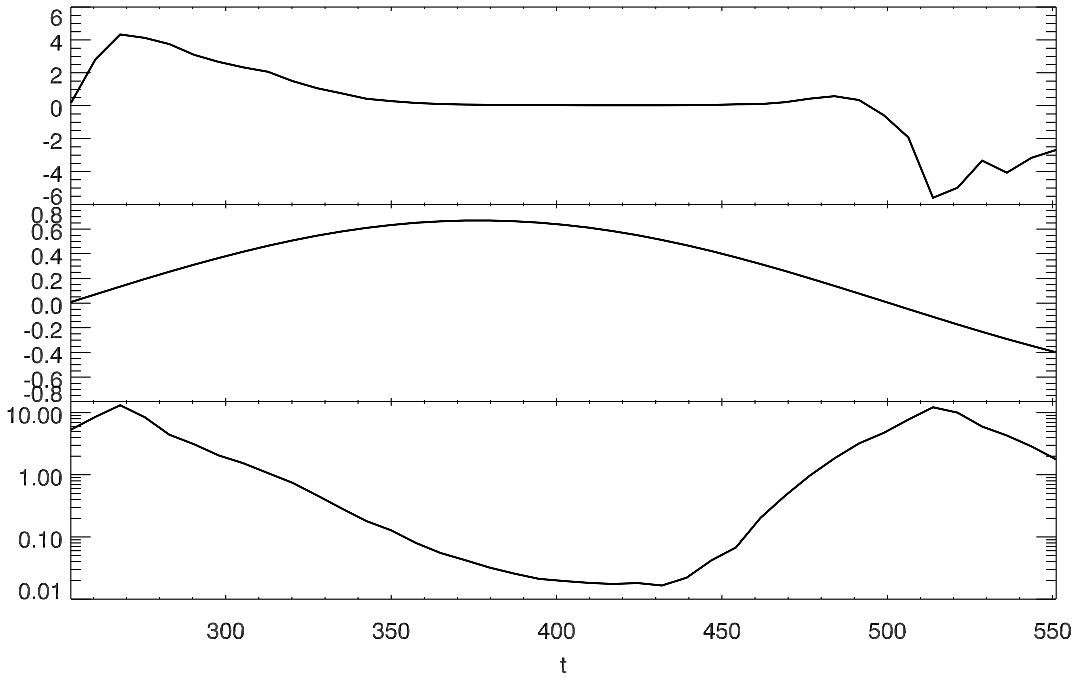

Fig. 2. Results of turbulence computation with cyclone base case parameters and artificial flow shear; parallel (braking) Reynolds stress (upper plot), shearing rate (middle plot), χ_i (lower plot), all in natural dimensionless units. For flow shears above 0.15, the braking parallel stress is decreasing in terms of absolute numbers. The RMS self-consistent flow shear is 0.28. (The initial rise in χ_i is due to the preceding negative half wave of the artificial flow.)

5 Transport of parallel momentum

Further investigation of the turbulent parallel force [16] shows that it is essentially due to the quasilinear diffusion of the parallel flow caused by the ambient ITG turbulence, and is of similar magnitude as the anomalous heat diffusion coefficient. In addition, different from the poloidal flow component, the parallel one is subject to an instability localized in the regions of maximum flow shear. For non-marginal ITG turbulence, however, the instability has much too low saturation amplitude to come up for the observed equilibrium braking force. To further corroborate the quasilinear nature of the parallel braking, we show the parallel Reynods stress for an artificially superposed flow in fig. 2. While it is braking in that case, too, it is decreasing with increasing flow shear. This is due to the reduction of the ambient ITG turbulence by the increasing flow shear, and is incompatible with stress being due to a genuine flow instability.

Poloidal and parallel stress behave different with respect to the ZF drive, because the turbulent structures can be effectively sheared by the poloidal velocity field whereas they cannot by the parallel velocity, due to the enormous anisotropy of the turbulent structures, which have perpendicular scale legths of order of about $10\rho_i$ but parallel scale lengths of order of the connection length, qR. The perpendicular flow shear is thus able to tilt the turbulent structures, so that the resulting turbulent stress amplifies the flow, while the parallel momentum is just redistributed by the turbulent eddies.

Moving away from the tokamak center, with rising safety factor q the importance of the parallel force on the flows increases strongly. This is because both the energy of the parallel flow component and the quasilinear diffusion coefficient for it increase proportional to q^2. (The parallel connection length affects the quasilinear parallel momentum diffusion coefficient through the ratio of parallel sound transit time to turbulence time scales.) This leads overall to an excessive parallel braking in the tokamak edge where $q \gtrsim 3$, which explains the complete quench of the stationary ZFs, leaving only the geodesic acoustic modes [4].

6 Conclusions

In a curved magnetic geometry the requirement of incompressibility couples quasi-stationary poloidal flows to parallel return flows, which, for average parameters, comprise the major part of the flows' free energy. Consequently, the behavior of quasi-stationary zonal flows depends crucially on the appropriate flux surface average of the parallel Reynolds stress and not alone on the perpendicular Reynolds stress. Different from the perpendicular flows the parallel ones tend to be damped by turbulence and are prone to instabilities. In numerical turbulence studies the parallel flow braking was found to be responsible for ZF saturation, while the poloidal flow component continues to be driven. For saturated turbulence states, the braking effect was found to be caused by the quasilinear transport of parallel momentum by the ambient ITG turbulence and not by the instability. The importance of the parallel stress is controlled mainly by the safety factor q because, on one hand, the energy in the parallel flow is proportional to q^2, and on the other hand, both the quasilinear parallel turbulence viscosity and the ZF instability threshold depend on the square of the sound frequency $\omega_S^2 \propto q^2$. On account of this strong dependence, safety factors of over three seem to completely suppress the stationary flows in fluid turbulence simulations leaving only the oscillating geodesic acoustic modes [4]. All these facts suggest the inclusion of the parallel return flow dynamics in analytical transport models [17]. Moreover, an experimental measurement of the forcing of the toroidicity induced flow component, e.g., by similar methods as in [5, 18] would seem very interesting.

References

[1] P. H. Diamond, M. N. Rosenbluth et al., 17th IAEA Fusion Energy Conference, IAEA-CN-69/TH3/1 (1998)

[2] K. H. Burrell, Phys. Plasmas **4** 1499 (1997)

[3] Z. Lin et al., Science **281**, 1835 (1998)

[4] K. Hallatschek, D. Biskamp, Phys. Rev. Lett. **86**, (2001) 1223

[5] C. Hidalgo et al., Phys. Rev. Lett. **83**, (1999) 2203

[6] B. N. Rogers, W. Dorland, M. Kotschenreuther, Phys. Rev. Lett. **85**, (2000) 5336

[7] K. Hallatschek, A. Zeiler, Phys. Plasmas **7**, (2000) 2554

[8] A. Zeiler, et al., Phys. Plasmas **5**, (1998) 2654

[9] F. L. Hinton, M. N. Rosenbluth, Plasma Phys. Control. Fusion **41**, (1999) A653

[10] M. N. Rosenbluth et al., Phys. Rev. Lett. **80**, (1998) 724

[11] T. S. Hahm, et al., Phys. Plasmas, **6**, (1999) 922

[12] K. Itoh, S. I. Itoh, Plasma Phys. Control. Fusion **38**, (1996) 1

[13] K. Hallatschek, Phys. Rev. Lett. **93**, 125001 (2004)

[14] A. M. Dimits, et al., Phys. Plasmas **7**, (2000) 969

[15] K. Hallatschek, Phys. Rev. Lett. **84**, 5145 (2000)

[16] K. Hallatschek, Phys. Rev. Lett. **93**, 65001 (2004)

[17] K. Itoh, K. Hallatschek, S. Toda, H. Sanuki, S-I Itoh, "Coherent structure of zonal flow and nonlinear saturation", J. Phys. Soc. Jpn. **73**, (2004), in press

[18] R. A. Moyer et al., Phys. Rev. Lett. **87**, (2001) 135001